Journal of Thermal Science Vol.31, No.5 (2022) 1266−1278

https://doi.org/10.1007/s11630-022-1694-6 **Article ID: 1003-2169(2022)05-1266-13**

CO_2 Plume Geothermal (CPG) Systems for Combined Heat and Power Production: an Evaluation of Various Plant Configurations

SCHIFFLECHNER Christopher*, WIELAND Christoph, SPLIETHOFF Hartmut

Chair of Energy Systems, TUM School of Engineering and Design, Technical University of Munich, 85747 Garching, Germany

Abstract: CO_2 Plume Geothermal (CPG) systems are a promising concept for utilising petrothermal resources in the context of a future carbon capture utilisation and sequestration economy. Petrothermal geothermal energy has a tremendous worldwide potential for decarbonising both the power and heating sectors. This paper investigates three potential CPG configurations for combined heating and power generation (CHP). The present work examines scenarios with reservoir depths of 4 km and 5 km, as well as required district heating system (DHS) supply temperatures of 70°C and 90°C. The results reveal that a two-staged serial CHP concept eventuates in the highest achievable net power output. For a thermosiphon system, the relative net power reduction by the CHP option compared with a sole power generation system is significantly lower than for a pumped system. The net power reduction for pumped systems lies between 62.6% and 22.9%. For a thermosiphon system with a depth of 5 km and a required DHS supply temperature of 70°C, the achievable net power by the most beneficial CHP option is even 9.2% higher than for sole power generation systems. The second law efficiency for the sole power generation concepts are in a range between 33.0% and 43.0%. The second law efficiency can increase up to 63.0% in the case of a CHP application. Thus, the combined heat and power generation can significantly increase the overall second law efficiency of a CPG system. The evaluation of the achievable revenues demonstrates that a CHP application might improve the economic performance of both thermosiphon and pumped CPG systems. However, the minimum heat revenue required for compensating the power reduction increases with higher electricity revenues. In summary, the results of this work provide valuable insights for the potential development of CPG systems for CHP applications and their economic feasibility.

Keywords: deep geothermal energy, combined heat and power generation, CO_2 plume geothermal systems, petrothermal resources, carbon capture, utilisation and storage

Article Type: Contributed by the International Conference on Efficiency, Cost, Optimization, Simulation & Environmental Impact of Energy Systems (ECOS 2021) GE: SUN Jie
Received: Oct 28, 2021 Corresponding author: SCHIFFLECHNER Christopher E-mail: c.schifflechner@tum.de

Nomenclature

Letter symbols

A	effective vertical cross-section of reservoir/m^2
D	diameter/m
e	exergy/$kJ \cdot kg^{-1}$
$\dot{E}x$	exergy flow rate/kW
f	Darcy factor
g	gravitational acceleration/$m \cdot s^{-2}$
h	enthalpy/$kJ \cdot kg^{-1}$
L	reservoir length interval/m
$\dot{m}$	mass flow rate/$kg \cdot s^{-1}$
P	electrical power/kW
p	pressure/kPa
$\dot{Q}$	heat flow/kW
R	ratio of the revenues
Re	Reynolds number
Rev	revenues/$EUR \cdot kWh^{-1}$
T	temperature/°C
t_0	reference temperature/K
V	velocity/$m \cdot s^{-1}$
z	well length interval/m

Greek symbols

Δ	difference
ε	pipe surface roughness/m
η	efficiency
κ	reservoir permeability/m^2
μ	dynamic fluid viscosity/$N \cdot s \cdot m^{-2}$
ρ	density/$kg \cdot m^{-3}$
ψ	surface exergy change/$kJ \cdot s^{-1}$

Subscripts

0	reference state
I	First law efficiency
II	Second law efficiency
av	average
DHS	district heating system
el	electric
fans	fans air-cooled condenser
f, well	friction within the well
in	inlet
inj	injection
net	net power
out	outlet
prod	production
pump	pump
pumped	pumped system
Res	reservoir
th	thermal
thermo	thermosiphon system
turb	turbine
WH	wellhead

Abbreviations

CCS	Carbon Capture and Storage
CCUS	Carbon Capture Utilisation and Sequestration/ Storage
CHP	Combined Heat and Power Generation
CPG	CO_2 Plume Geothermal
DHS	District Heating System
EGS	Enhanced Geothermal Systems
ORC	Organic Rankine Cycle
SPG	Sole Power Generation

1. Introduction

1.1 Background

Deep geothermal energy could play a major role in the decarbonisation of the power, heating and cooling sector [1]. It has a tremendous worldwide technical potential, as reported by Aghahosseini et al. [2]. Currently, most of the existing geothermal projects use hydrothermal reservoirs. While this concept has a high technology-readiness level, the presence of hydrothermal resources is limited to certain favourable geological regions. For example, it is estimated that hydrothermal reservoirs contain only about 5% of Germany's countrywide technical potential of deep geothermal energy [3]. Thus, an increased focus on petrothermal projects will be needed if deep geothermal energy is to contribute to the necessary transformation of the energy system on a global scale in coming decades. The recent work by Pan et al. [4] presents the state-of-the-art information on enhanced geothermal projects (EGS) and discusses the potential challenges and barriers for future EGS projects. Any increased willingness on the part of potential investors investing in petrothermal projects will call for an improved thermodynamic and economic performance [5]. Benim et al. [6] present a detailed investigation of the thermohydraulics of an EGS project. Gao et al. [7] propose a novel horizontally layered EGS system that could provide a significantly higher heat power output than a classic double vertical well EGS.

The conventional utilisation concept of petrothermal energy foresees the use of water as a heat carrier medium. Power generation takes place either by a direct or an

indirect binary power plant concept, depending on the achievable water temperatures [8].

However, the use of CO_2 as a heat carrier has attracted growing interest by academia and industry in the last 20 years, and the results of a first larger research demonstration project have recently been published [9]. Brown [10] describes several promising advantages of using CO_2 as a potential heat carrier compared to water. Firstly, even at low reservoir depths, the CO_2 can be used directly within a turbine for power generation. Secondly, the high-density variation of CO_2 causes a strong buoyancy effect, which results in a high self-driven mass flow rate without the need for a pump – a so-called thermosiphon. Finally, CO_2 has a lower kinematic viscosity and a lower salt solubility than water. Randolph and Saar [11] developed the concept further combining the geothermal energy production with geological carbon dioxide sequestration. The authors named their concept CO_2 plume geothermal (CPG) system and distinguish their approach from CO_2 based EGS systems. Adams et al. [12] provide a detailed critical evaluation of water and CO_2 as heat carriers for geothermal power production. Garapati et al. [13] also demonstrate that the combination of a CPG system with other heat sources can result in a promising hybrid concept for power generation. Next to the promising system characteristic itself, CPG systems might be a favourable technology within a future context of carbon capture and storage (CCS) [14] and in a carbon capture utilisation and sequestration/storage (CCUS) economy [15].

While the thermosiphon effect is one of the main drivers for considering CO_2 as a heat carrier, several studies suggest that a pumped CO_2 system could achieve even higher net power outputs. For example, both Refs. [12] and [16] reveal that a pumped CO_2 system can significantly increase the net power especially for deep reservoirs. Hansper et al. [16] report an 18% higher net power for the pumped system. Adams et al. [12] highlight that the achievable net power increase of a pumped system depends on the reservoir depth. While the increase is rather small for reservoir depths below 3 km, a net power increase of more than 40% can be observed for a reservoir depth of 5 km.

Whereas there is an increasing number of publications regarding the sole power generation of CPG systems, their potential role for combined heat and power generation (CHP) has so far only been considered in a limited number of studies. The sole power generation is a reasonable application case for geothermal projects in areas with low population density. However, as described by Goetzel et al. [17], deep geothermal energy might play a significant role within the transition and decarbonising of district heating systems. For example, Refs. [18], [19] and [20] evaluated various plant designs for deep geothermal CHP or polygeneration systems with water as heat carrier. Therefore, CPG systems should also be assessed against the background of their applicability for CHP concepts. However, only very few studies so far focus on the CHP applications of CPG systems. Gladysz et al. [21] and [22] investigate a two-staged serial concept for a potential CPG project in Poland. Schifflechner et al. [23] compare the performance of a CPG system with a water-Organic Rankine Cycle (ORC) system for a CHP application, while proposing a combined serial-parallel concept for the CPG system.

1.2 This paper's contribution

Consequently, while the existing papers provide an initial and valuable insight into potential CHP concepts for CPG systems, there is still a lack of a detailed comparison of different CHP concepts for various application scenarios. Therefore, this paper makes a valuable contribution by comparing the performance of several CHP plant concepts. The evaluation is carried out for different reservoir depths and required district heating system (DHS) supply temperatures. Finally, an assessment of the achievable operating earnings, depending on the electricity and heat revenues is made. This makes it possible to draw conclusions about the minimum required heat tariff prices at which a CHP concept might be economically beneficial compared to a sole power generation project. In summary, the results of this work provide valuable insights for the potential development of CPG systems for CHP applications, as well as assessing their economic feasibility.

2. Methods

The following section describes the overall CPG system and its simulation model, as well as the system parameters considered.

2.1 System description

The overall concept of a CPG system for sole power generation and the corresponding T,s-diagram are visualized in Fig. 1. The inlet conditions of the production well are determined by the depth of the reservoir and the geothermal gradient. Both the pressure and temperature of the CO_2 decrease within the production well. Since the CO_2 has gas-like properties within the well, the decrease in enthalpy mainly affects the temperature compared to a liquid-like water system. A more detailed discussion of the effect is presented in Refs. [10, 12, 24]. Thus, the CPG system can achieve significantly higher wellhead pressure conditions than water, which is favourable for the direct power generation within a turbine. However, the wellhead temperature of the CO_2 is significantly lower than for a

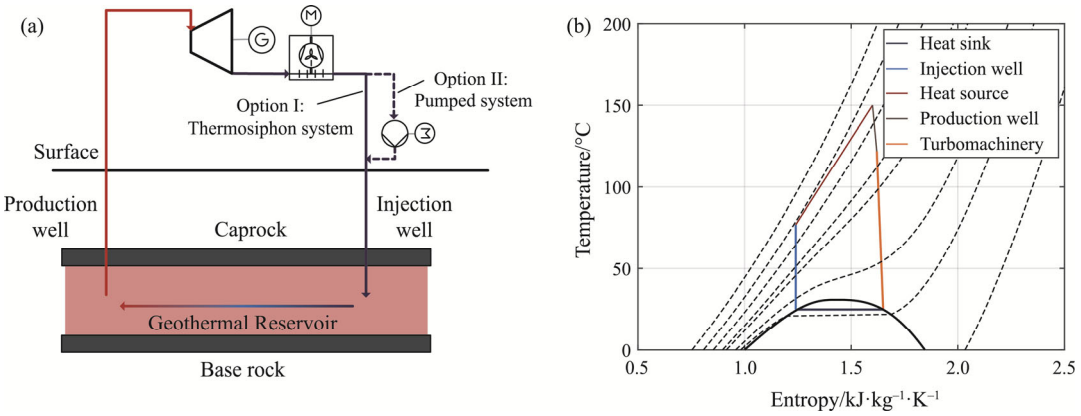

Fig. 1 (a) Simplified visualisation of a CPG system and (b) its corresponding *T*,*s*-diagram for a thermosiphon system

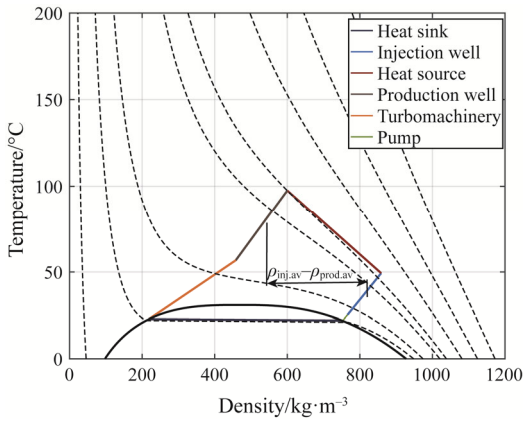

Fig. 2 Temperature-density diagram of a pumped CPG system

water system. Thus, for CHP applications, deeper reservoirs will be necessary for CPG systems to achieve the required DHS supply temperature. In the next step, the CO_2 expands directly within the turbine. After this expansion, the CO_2 is cooled down and (depending on the pressure level) condensed. This step is required to ensure a sufficient density variation between the cold injection and the hot production well, which is the pivotal driving force for the positive thermosiphon effect [25]. The temperature depended density variation and thermal expansibility of CO_2 is significantly higher compared with water [25, 26]. Fig. 2 visualizes the CPG process within a temperature-density diagram of CO_2. The figure highlights the significant variation of the CO_2 density between the injection and production well. The substantial density difference causes a high pressure difference within the system, which drives the CO_2 thermosiphon [25]. The strong thermosiphon effect is further enhanced by low kinematic viscosity of CO_2 compared with water. Thus, no further equipment is required for such a CO_2 thermosiphon system. In the case of a pumped system, the pressure is increased by an above-ground pump before the CO_2 enters the injection well.

2.2 System modelling

The system is modelled using MATLAB R2019b [27] and REFPROP 10.0 [28] as a database for the fluid properties of CO_2. The wells are modelled by the methodology described in detail by Atrens et al. [29] and Adams et al. [12]. Within the wells, the property changes of the CO_2 are calculated iteratively for length intervals of Δz=50 m. Steady-state operation and a lack of heat flow across the well boundaries are assumed (cf. [12, 24, 29]). Subsequent formulas determine the pressure drop Δp within one well segment due to change in hydrostatic pressure and friction within the well. $\Delta p_{\mathrm{f,well}}$ represents the pressure drop within one segment due to friction; f is the Darcy friction factor; Δh is the change in the fluid enthalpy, V the fluid velocity and ε the well roughness.

$$\Delta p = \rho g \Delta z - \Delta p_{\mathrm{f,well}} \tag{1}$$

$$\Delta p_{\mathrm{f,well}} = f \frac{\Delta z \rho}{D} \frac{V^2}{2} = f \frac{8 \dot{m}^2 \Delta z}{\pi^2 \rho D^5} \tag{2}$$

$$f = \left\{ -1.8 \log_{10} \left[\frac{6.9}{Re} + \left(\frac{\varepsilon}{3.7D} \right)^{1.11} \right] \right\}^{-2} \tag{3}$$

$$\Delta h = g \cdot \Delta z - \frac{\Delta \left(V^2 \right)}{2} \tag{4}$$

Based on the previous equations and the defined reservoir pressure p_{Res}, the pressure at the wellhead p_{WH} is calculated using following equation:

$$p_{\mathrm{WH}} = p_{\mathrm{Res}} - \rho g \Delta z - \Delta p_{\mathrm{f,well,prod}} \tag{5}$$

Darcy's law for a steady, laminar 1D flow through a porous medium calculates the pressure drop within the reservoir [12, 22]. A length interval ΔL of 50 m is considered.

$$\Delta p_{\mathrm{Res}} = \left(\frac{\mu \Delta L}{\rho A_{\mathrm{Res}}} \right) \frac{\dot{m}}{\kappa_{\mathrm{Res}}} \tag{6}$$

The subsequent formula was used for the thermosiphon system to determine the necessary

injection pressure [21]. A condensation pressure of at least 50 kPa above the condensation pressure for 22°C is assumed in the case of a pumped system [12].

$$p_{\mathrm{inj}} = p_{\mathrm{Res}} - \rho g \Delta z + \Delta p_{\mathrm{Res}} + \Delta p_{\mathrm{f,well,inj}} \tag{7}$$

The electrical net power $P_{\mathrm{el,net}}$ for the thermosiphon and pumped system are calculated using the following two equations:

$$P_{\mathrm{el,net,thermo}} = P_{\mathrm{el,turb}} - P_{\mathrm{el,fans}} \tag{8}$$

$$P_{\mathrm{el,net,pump}} = P_{\mathrm{el,turb}} - P_{\mathrm{el,fans}} - P_{\mathrm{el,pump}} \tag{9}$$

Next to the sole power generation, three CHP configurations are investigated for both the thermosiphon and pumped systems. Fig. 3 shows the different plant layouts. A schematic *T*,*s*-diagram of the different CHP configurations is visualized in Fig. 4. The evaluated plant configurations are:

Sole power generation (SPG): The CO_2 is directly expanded within the turbine for sole power generation purposes. After the turbine outlet, an air-cooler cools and – depending on the turbine outlet pressure – condenses the CO_2. The reinjection pressure for the thermosiphon system is determined with Eq. (7) and also defines the turbine outlet pressure.

CHP Option I–simple serial concept: The CO_2 passes through the heat exchanger before entering the turbine. A minimum necessary pinch-point temperature difference of 5 K is assumed.

CHP Option II–two-staged serial concept: This concept was proposed initially by Gladysz et al. [21]. The CO_2 is expanded in a first turbine stage. The outlet pressure of this stage is regulated by the DHS supply temperature required and the defined minimum pinch-point temperature difference of 5°C. After the heat exchanger, the CO_2 is expanded in a second turbine stage. This option is only applied if the potential pressure difference for the first stage is at least 15% of the overall available pressure difference.

CHP Option III–combined serial-parallel concept: This concept was proposed by Schifflechner et al. [30]. The CO_2 is divided into two streams at the surface. One stream enters the turbine directly, while the second stream first passes through a heat exchanger before entering the turbine. The mass flow of path I is determined by the minimum pinch-point temperature of the heat exchanger. The CHP Option III is only applied if the achievable mass flow rate for path II is at least 15% of the overall mass flow rate.

As discussed critically in Ref. [23], the evaluation of geothermal CHP concepts typically requires a consideration of part-load behaviour, as well as a focus of the annual achievable net power, since the heating demand of a DHS varies strongly over a year. Although Gabrielle's model [31] provides a part-load model as a function of the working fluid's density, the work by Dawo et al. [32] indicates that this model may provide overly optimistic results for use with large-scale turbines in geothermal applications. Thus, the application of the part-load model by Ref. [31] would provide only very

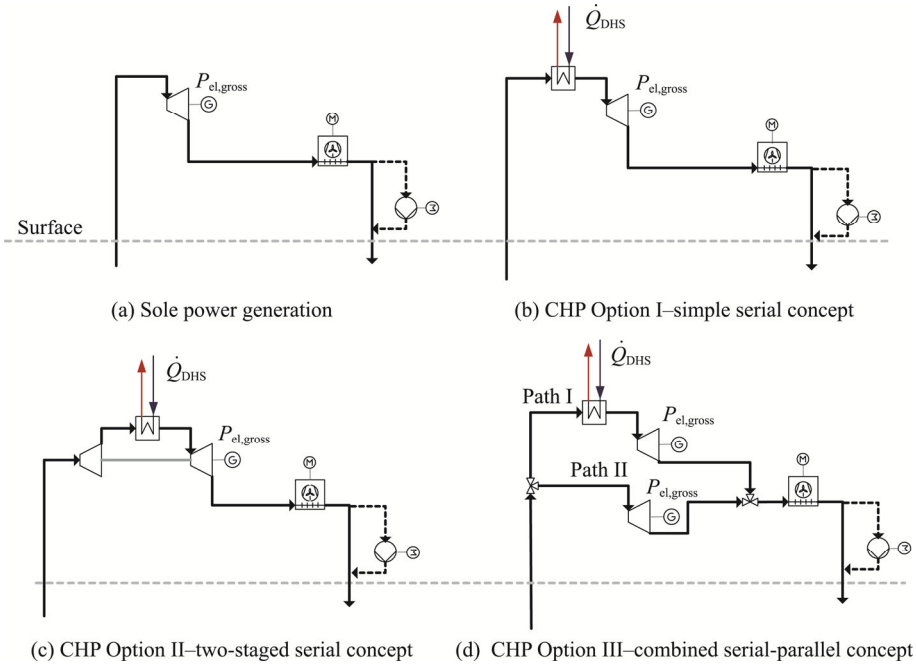

Fig. 3 Layout of the analysed configurations of the above-ground system. Layout (a) Sole power generation; layout (b) CHP Option I–simple serial concept; layout (c) CHP Option II–two-staged serial concept; Layout (d) CHP Option III–combined serial-parallel concept

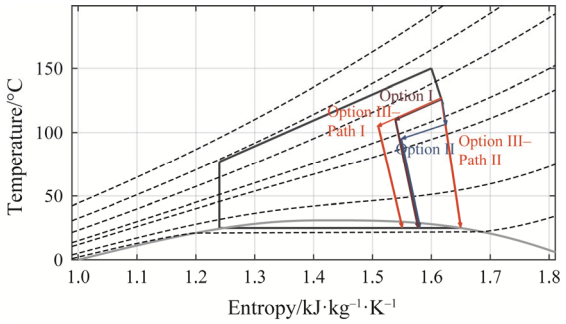

Fig. 4 Visualization of the three different CHP options in a *T*,*s*-diagram for a thermosiphon system

limited additional insights, since the part-load effects occurring would be negligible. Nevertheless, this work presents a valuable contribution, since it allows a detailed critical evaluation of several potential CHP plant layout concepts for different application scenarios but it needs to be considered that the analysis is only for a steady-state operation and neglects potential part-load effects.

2.3 System parameters

While several studies, such as that of Adams et al. [12], demonstrate that sole power generation by CPG systems is already feasible for low reservoir depths, this work assumes a depth of at least 4 km. This is necessary to ensure that the required heat demand and DHS supply temperature can be provided in every scenario. The assumed heat demand of the DHS is 20 MW_{th}, which is the average installed capacity for existing hydrothermal geothermal CHP projects in Germany [3]. Two different required temperature levels for the DHS are evaluated. One scenario is with a required DHS supply temperature of 90°C, which characterises an average value of existing DHS, and an alternative scenario with 70°C, which characterises a more modern network with a lower required supply temperature (cf. [33]). The further model parameters are taken from Refs. [12, 21, 23, 24]. Table 1 summarises the main model parameters.

2.4 Evaluation parameters

There are several potential suitable performance indicators for a meaningful evaluation of the investigated concepts. Most existing studies on CPG systems evaluate mainly the achievable electrical net power (cf. [12, 16]). This parameter is mainly relevant for the potential power capacity and achievable economics of a future CPG system. Nevertheless, an additional thermodynamic evaluation provides further useful insights especially with respect to the comparison of the different plant configurations. For the comparison of the two sole power generation concepts (thermosiphon and pumped system), the energetic first-law efficiency might be a suitable evaluation criterion:

Table 1 Summary of the main model parameters.

Parameter	Value
Depth	4 km; 5 km
Well diameter	0.33 m
Well roughness	55 µm
Permeability	5×10^{-14} m^2
Reservoir length	700 m
Reservoir thickness	300 m
Geothermal gradient	35°C/km
Reservoir temperature	155°C (4 km); 190°C (5 km)
Reservoir pressure	40 MPa (4 km); 50 MPa (5 km)
Isentropic turbine efficiency	0.78
Minimal required vapour quality at the turbine outlet	0.75
Isentropic pump efficiency	0.8
Heat demand	20 MW_{th}
DHS return and supply temp.	60°C–90°C; 40°C–70°C
Relative pressure drop in the heat exchanger for the DHS	0.5%
Pinch-Point temp. condenser	3°C
Ambient air temperature	15°C
Electricity demand of the fans	0.15 kW per kg·s^{-1} of air flow

$$\eta_{\mathrm{I}} = \frac{P_{\mathrm{el,net}}}{\dot{Q}_{\mathrm{Res}}} \tag{10}$$

However, since the main objective of this work is the evaluation of CHP systems, the exergetic second law efficiency should be considered [23, 34].

$$\eta_{\mathrm{II}} = \frac{P_{\mathrm{el,net}} + \dot{E}x_{\mathrm{DHS}}}{\psi} \tag{11}$$

The exergy flow related to the DHS $\dot{E}x_{\mathrm{DHS}}$ is calculated by subsequent formula for a reference temperature t_0 of 288 K [34].

$$\begin{aligned}\dot{E}x_{\mathrm{DHS}} &= \dot{m}_{\mathrm{DHS}} \times \left(e_{\mathrm{DHS,out}} - e_{\mathrm{DHS,in}}\right) \\ &= \dot{m}_{\mathrm{DHS}} \times \left[h_{\mathrm{DHS,out}} - h_{\mathrm{DHS,in}} - t_0 \right. \\ &\quad \left. \times \left(s_{\mathrm{DHS,out}} - s_{\mathrm{DHS,in}}\right)\right]\end{aligned} \tag{12}$$

As suggested by Atrens et al. [29] the surface exergy change ψ is determined by following equation:

$$\psi = \dot{m}_{\mathrm{CO_2}} \times \left[h_{\mathrm{WH}} - h_{\mathrm{inj}} - t_0\left(s_{\mathrm{WH}} - s_{\mathrm{inj}}\right)\right] \tag{13}$$

2.5 Model validation

The following section describes the validation of the base model to confirm the accuracy of the developed MATLAB model. This ensures that the reader can comprehend the later results in terms of their possible deviation with other data sources. The validation of the model focuses on two main aspects: First, the modelled

influence of the CO_2 mass flow on the achievable turbine power and the available pressure difference is to be validated. This is necessary to ensure that the model is reliably able to model the influence of different mass flow rates and thus identify the optimal CO_2 flow rate. Secondly, the validation of the results of a pumped system for a given mass flow is carried out to ensure that the determined values for the turbines and pumping power are plausible.

The model is validated with the data from Adams et al. [12], since this paper is published together with detailed supplementary data, which allows an exact validation of several parameters, such as the achievable net power out or the required pump power. The presented calculated results are obtained for the same model parameters described in Ref. [12]. First, the turbine pressure differential and gross turbine power output are validated by using the results shown in Fig. 5 for the base-case thermosiphon system of Adams et al. [12]. The comparison with the own results is visualized in Fig. 4. The results confirm that the deviation of both parameters is within a range below 5%. A small deviation between the calculations and the reported results appears to be acceptable considering that different sources are used for the property data of CO_2 and different simulation tools are applied. In the next step, the achievable turbine power $P_{\mathrm{el,turbine}}$, the required pump power $P_{\mathrm{el,pump}}$, and the extracted heat from the reservoir $\dot{Q}_{\mathrm{Res}}$ are validated. This is done for a reservoir depth of 3500 m, a mass flow rate of 140 kg/s and assumed injection and production pipe diameters of 0.33 m and 0.27 m respectively. More information about the assumptions and the reported results are listed in both Table 2 of Adams et al. [12] and in line 485 of the Excel file within the supplementary data of Adams et al. [12]. The comparison between the reported results and the calculated values is listed in Table 2. The results highlight that the relative deviation of the most crucial system parameters are between 0.7% and 1.5%, which can be seen as acceptable. Thus, it is assured that the developed model for this paper provides reasonable and accurate results.

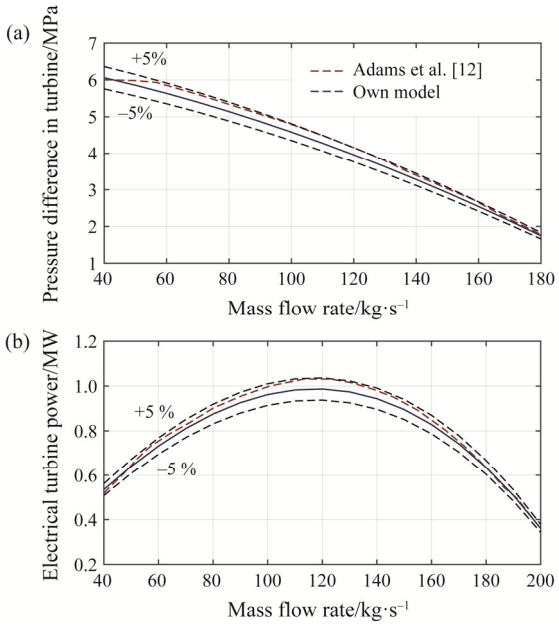

Fig. 5 Model validation for varying mass flow rates: (a) comparison of the pressure difference in the turbine and (b) its resulting electrical turbine power

Table 2 Summary of the main model parameters

Parameter	Adams et al. [12]	Own model	Relative deviation
$P_{\mathrm{el,turbine}}$	3145 kW	3123 kW	–0.70%
$P_{\mathrm{el,pump}}$	–690 kW	–674 kW	–1.23%
$\dot{Q}_{\mathrm{Res}}$	21 638 kW	21 969 kW	+1.53%

3. Results

This section describes and discusses the obtained results. Firstly, the results for sole electricity generation are presented, before the CHP performance is evaluated. Afterwards, an estimation of the minimum required heat revenues for an economic CHP operation is determined.

3.1 Sole power generation

Based on the previous presented system parameters, the achievable electrical net power in the case of sole power generation is assessed as a reference scenario for the later evaluation of the CHP scenarios. The achievable electrical net power for depths of 4 and 5 km for both the thermosiphon and pumped system are visualised in Fig. 6. The results reveal that an optimal mass flow with a maximum net power output occurs for all the cases investigated, which aligns with the results reported in other studies such as that by Adams et al. [12] or Hansper et al. [16]. The occurrence of an optimum can mainly be explained by two factors. Firstly, the available pressure difference between the turbine inlet and outlet pressure decreases for higher mass flow rates. Thus, the specific mass flow rate power output decreases for increasing mass flow rates. Secondly, the required auxiliary power for the air fans and the pump increases even further with a higher mass flow. Therefore, from a certain optimum point on, the achievable net power decreases for higher mass flow rates. Fig. 6(b) shows that the optimal mass flow rate of the pumped system is significantly higher than for the thermosiphon system. The different turbine outlet pressure mainly causes this effect. For the thermosiphon system, the required turbine outlet pressure increases significantly for higher mass flow rates, resulting in a lower mass specific power output. For a pumped system, the turbine outlet pressure remains mainly constant. Hence, for a pumped system the effect

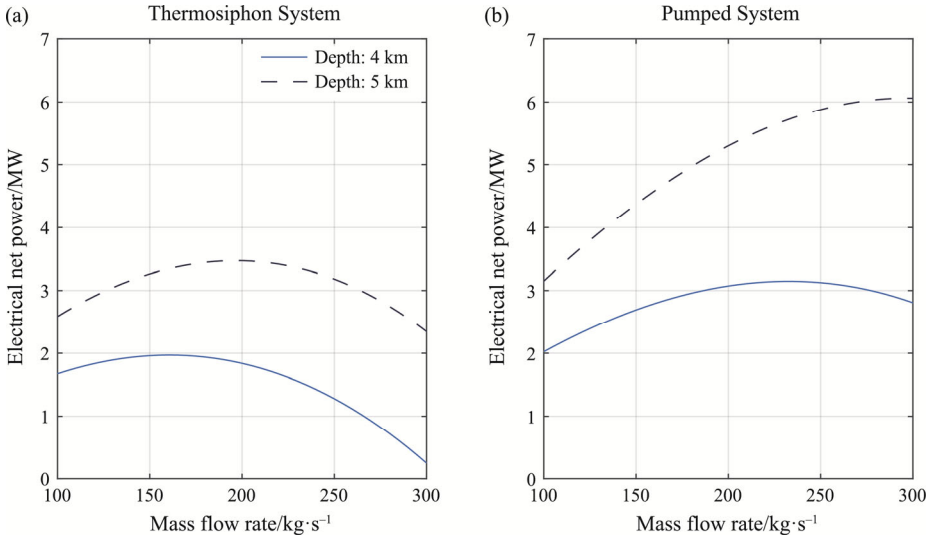

Fig. 6 Achievable net power for various mass flow rates for (a) a thermosiphon system and (b) a pumped system

of a power decrease for higher mass flow rates by the lower wellhead pressure and the higher required power for the condenser occurs at higher flow rates compared with a thermosiphon system.

In addition, Fig. 6 highlights the strong effect of the reservoir depth on the achievable net power. Comparing the 5 km depth with a depth of 4 km reveals that the achievable power is 76% higher for the thermosiphon system and 92% higher for the pumped system. The application of a pump can increase the net power output up to 75%. Fig. 7 compares the gross and net power output for both analysed systems and reservoir depths. It depicts the four scenarios with the maximum net power output shown in Fig. 6. In the case of a pumped system, the achievable gross outputs are more than twice as high as for the thermosiphon system. However, due to the pump's high electricity demand, the net power increases are only 59% and 75%, respectively.

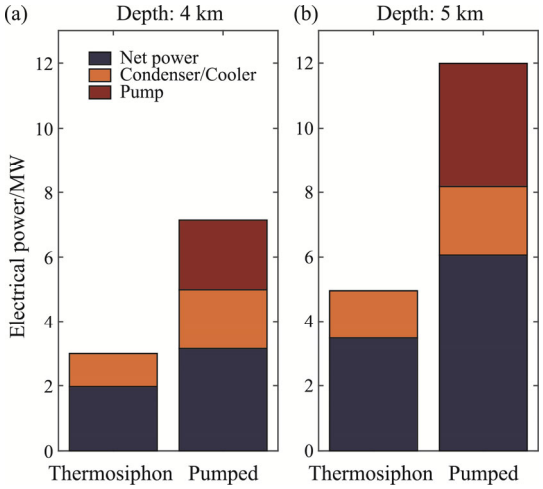

Fig. 7 Comparison of the highest achievable gross and net power output for (a) a depth of 4 km and (b) 5 km

3.2 Combined heat and power generation

Fig. 8 reveals the achievable net power for the CHP concepts investigated, considering a reservoir depth of 5 km and required DHS supply temperature of 90°C. For the thermosiphon system, the optimal mass flow rate is higher in the case of a CHP application, while the overall achievable net power is lower than for a sole power generation system. Option II achieves the highest net power output. The simple serial concept (Option I) results in the lowest power output. This order applies also for the pumped system. However, the power reduction in the case of a CHP application is significantly higher for the pumped system. This can be mainly explained by two effects. Firstly, due to the fluid properties of CO_2, the available enthalpy difference for the power generation within the turbine decreases significantly with lower turbine inlet temperatures, even if the pressure difference between turbine inlet and outlet remains the same. Thus, the negative effect of the cooled CO_2 is more significant than in the case of the thermosiphon system due to the higher pressure difference within the turbine. Secondly, the vapour quality at the turbine outlet would be below the defined minimal value of 0.75 for many mass flow rates. Therefore, a slightly higher turbine outlet pressure is required to meet this criterion, which further reduces the turbine power output. The results obtained for the net power output for both the thermosiphon and pumped systems are listed in Tables 3 and 4. Due to the low CO_2 wellhead temperature of 100°C in the case of 4 km reservoir depths, only CHP Option I is feasible based on the assumed necessary minimal pinch-point temperature for the DHS heat exchanger.

Table 5 describes the relative change of the achievable net power between the optimal CHP configuration and a SPG project. The results demonstrate that the power

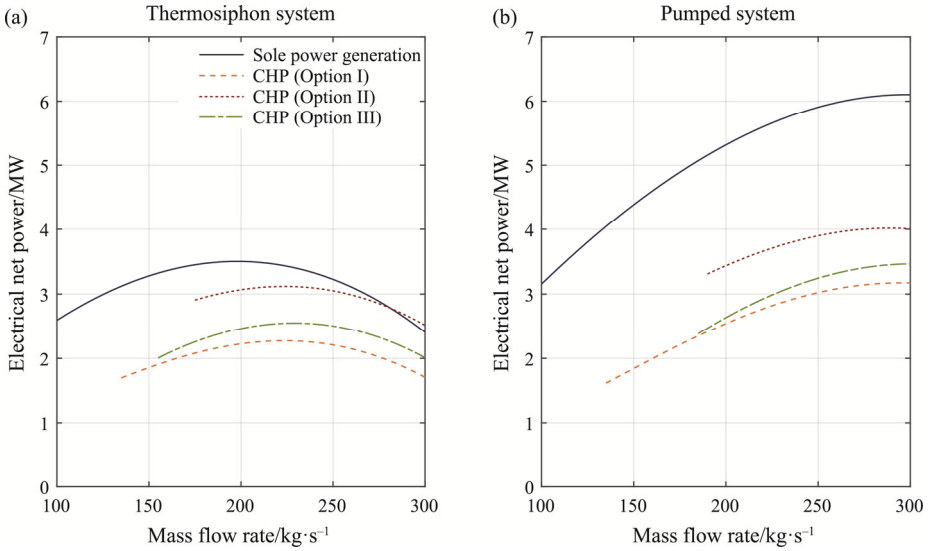

Fig. 8 Achievable net power for (a) a thermosiphon system and (b) a pumped system at a depth of 5 km and where a supply temperature of 90°C for the district heating network is required.

Table 3 Achievable net power for different depths, and the district heating supply and return temperatures for a thermosiphon system

System	4 km Depth		5 km Depth	
Temperature/°C	60–90	40–70	60–90	40–70
Sole power generation	1.97 MW	1.97 MW	3.47 MW	3.47 MW
CHP–Option I	1.16 MW	1.19 MW	2.25 MW	2.25 MW
CHP–Option II	–	1.76 MW	3.10 MW	3.79 MW
CHP–Option III	–	1.40 MW	2.53 MW	2.73 MW

Table 4 Achievable net power for different depths, and the district heating supply and return temperatures for a pumped system

System	4 km Depth		5 km Depth	
Temperature/°C	60–90	40–70	60–90	40–70
Sole power generation	3.14 MW	3.14 MW	6.06 MW	6.06 MW
CHP–Option I	1.21 MW	1.21 MW	3.14 MW	3.14 MW
CHP–Option II	–	1.77 MW	3.97 MW	4.67 MW
CHP–Option III	–	1.34 MW	3.42 MW	3.83 MW

Table 5 Relative change in the achievable net power reduction of the most beneficial CHP option compared to the SPG scenario

System	4 km Depth		5 km Depth	
Temperature/°C	60–90	40–70	60–90	40–70
Thermosiphon system	–42.1%	–11.2%	–10.7%	+9.3%
Pumped system	–62.6%	–43.4%	–34.5%	–22.9%

reduction in the case of CHP configuration decreases for a lower required DHS supply temperature. One interesting special case is the thermosiphon system for the scenario with 5 km depth and a required DHS supply temperature of 70°C. In this scenario, the net power from the most beneficial CHP option is 9.2% higher than in the case of SPG. Due to the low required temperature level, the outlet pressure of the first turbine stage is rather low, resulting only in a minor gross power reduction. Furthermore, as for all CHP concepts, the required auxiliary power demand of the air-cooled condenser is reduced. Thus, the combination of both effects leads to a slightly higher net power than for the sole power generation, as shown in Fig. 9.

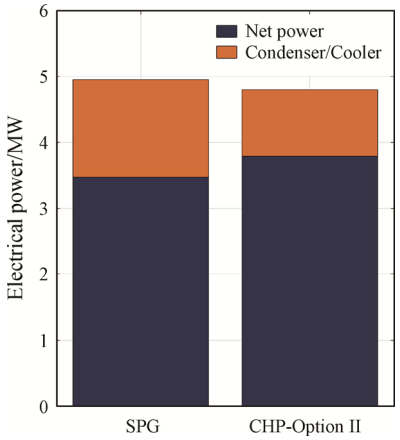

Fig. 9 Comparison of the gross and net power output between the sole power generation (SPG) and the most beneficial CHP option for a depth of 4 km and DHS supply temperature of 70°C

3.3 First and second law evaluation

In the first step, the thermodynamic first law efficiency of the sole power generation concept is evaluated for both the different investigated reservoir depths and the thermosiphon and pumped configuration.

The results are reported in Table 6. The thermal efficiency varies between 6.5% for the 4 km thermosiphon system and 8.8% for the 5 km pumped system. Table 6 displays that the pumped systems result a slightly higher first law efficiency and that the efficiency increases for both concepts in the case of a higher reservoir depth. Both, the range and behaviour of the results correspond with reported data from other researchers, such as Hansper et al. [16].

The second law efficiencies for the mass flow rates with the highest achievable net power output are listed in Table 7 for the thermosiphon and pumped system respectively. The second law efficiency for the sole power generation concepts are in a range between 33.0% and 43.0%. Again, the range of these results is in line with the findings of other researchers (cf. [16]). The second law efficiency can increase up to 63.0% in the case of a CHP application. Thus, the combined heat and power generation can significantly increase the overall second law efficiency of a CPG system compared with a sole power generation concept. This effect is also reported for other geothermal CHP systems with water as a heat carrier [34]. While the fist law efficiency is higher for the pumped system, the thermosiphon systems obtain slightly higher second law efficiencies in the case of combined heat and power generation. Comparing the different CHP options reveals that in the case of the 5 km depth, Option II displays both the highest obtained net power output and the highest second law efficiency.

Table 6 First law efficiency of the sole power generation concept for different reservoir depths

Depth	Thermosiphon	Pumped
4 km	6.49%	6.93%
5 km	7.77%	8.82%

Table 7 Second law efficiency of the thermosiphon and pumped system for 4 and 5 km reservoir depth and a DHS supply temperature of 90°C

System	4 km Depth		5 km Depth	
	Thermo.	Pumped	Thermo.	Pumped
Sole power generation	32.95%	39.06%	33.79%	43.00%
CHP–Option I	62.98%	60.91%	50.10%	46.60%
CHP–Option II	–	–	57.54%	53.82%
CHP–Option III	–	–	50.69%	48.13%

3.4 Economic evaluation of the achievable revenues during operation

Based on the derived performance parameters, the following section evaluates the achievable earnings during operation for the most beneficial CHP configuration compared with a system for sole power generation (SPG). Consequently, the revenues for the most promising CHP concept are compared with the revenues in the case of a SPG project. The $R_{\text{CHP to SPG}}$ factor compares the earnings obtained from both concepts during operation.

$$R_{\text{CHP to SPG}} = \frac{P_{\text{el,net,CHP}} \cdot \text{Rev}_{\text{el}} + Q_{\text{th,CHP}} \cdot \text{Rev}_{\text{th}}}{P_{\text{el,net,SPG}} \cdot \text{Rev}_{\text{el}}}$$

if $R_{\text{CHP to SPG}} > 1$: higher revenues for the CHP case (14)

if $R_{\text{CHP to SPG}} < 1$: higher revenues for the SPG case

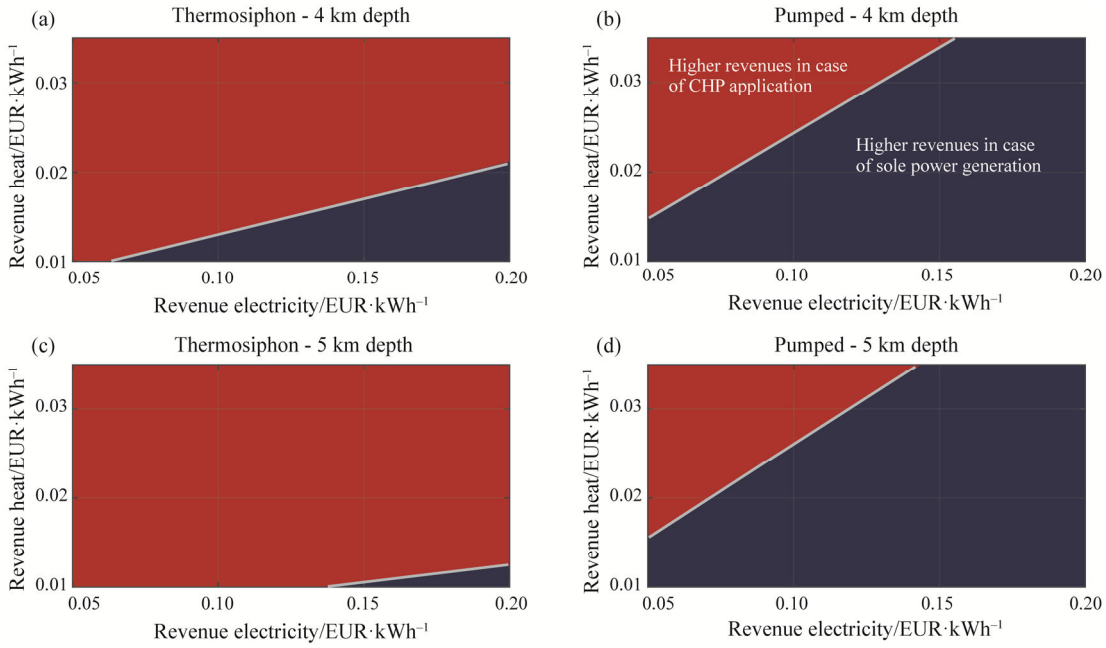

Fig. 10 Comparison of the achievable revenues for various heat and electricity revenues for a DHS with a supply temperature of 90°C

Fig. 10 presents a favourability map for the different reservoir depths and CPG concepts in the case of a required DHS supply temperature of 90°C. The red area indicates potential combinations of heat and electricity revenues, resulting in higher earnings in the case of a CHP application. The necessary minimum value for the heat revenues increases for higher electricity revenues. Thus, the potential economic advantageousness of a CHP concept will be strongly affected by the locally achievable revenues for both power and heat.

Eyerer et al. [3] assume heat revenues of 0.03 EUR/kWh$_{th}$ for existing geothermal CHP projects in Germany. At this potential heat selling price[1], pumped systems could also achieve higher earnings if the electricity revenue is below 0.125 EUR/kWh$_{el}$. This highlights the fact that CHP systems might be a promising concept for improving the economic performance of a CPG system, despite their significant power reduction for pumped systems. If lower DHS supply temperatures are required, CHP concepts would further improve profitability.

4. Conclusions and Outlook

The performance of three different CHP configurations for CPG systems are evaluated in this paper. The summarised key findings are:

(1) CPG systems are suitable for CHP applications, but they need larger reservoir depths than systems with water as a heat carrier medium. Nevertheless, from a depth of 4 km on, CPG systems can supply DHS with today's usual required temperature levels. With the expected future reduction of the supply temperatures in DHS, also CPG systems with lower depths will be eligible for CHP applications.

(2) The evaluation of three CHP configurations reveals that the two-staged serial concept (Option II) results in the highest achievable net power output. However, it requires a wellhead temperature that is significantly above the required DHS supply temperature. Thus, for a reservoir depth of 4 km and a required DHS supply temperature of 90°C, only CHP Option I is feasible.

(3) For a thermosiphon system, the relative net power reduction by the CHP option is significantly lower than for a pumped system. The net power reduction for pumped systems lies between 62.6% and 22.9%.

(4) For a thermosiphon system with 5 km depth and a required DHS supply temperature of 70°C, the achievable net power by the most beneficial CHP option is 9.2% higher than in the case of sole power generation.

(5) The thermal efficiency in the case of sole power generation varies between 6.5% for the 4 km thermosiphon system and 8.8% for the 5 km pumped system. The second law efficiency for the sole power generation concepts are in a range between 33.0% and 43.0%. The second law efficiency can increase up to 63.0% in the case of a CHP application. Thus, the combined heat and power generation can significantly increase the overall second law efficiency of a CPG system. Comparing the different CHP options reveals that in the case of the 5 km depth, Option II displays the highest obtained net power output and the highest second law efficiency.

(6) The evaluation of the achievable earnings demonstrates that a CHP application might improve the economic performance of a CPG system. Especially for thermosiphon systems, significant revenue increases can be achieved in most scenarios for heat revenues higher than 0.015 EUR/kWh$_{th}$. For a heat revenue of 0.03 EUR/kWh$_{th}$ pumped systems could achieve higher earnings, presupposed that the electricity revenue is below 0.125 EUR/kWh$_{el}$. For DHS supply temperatures that need to be lower than 90°C, the expected profitability of CHP projects would improve even further.

The results of this work provide valuable insights into the potential development of CPG systems for CHP applications, as well as an assessment of their economic feasibility. Based on this work, further studies could be carried considering several currently neglected effects and potential challenges for a practical implementation of CPG-CHP systems: The applicability of CO_2 as a heat carrier for CHP systems depends mainly on the required supply temperature of the district heating system. The study reveals that a supply temperature of 90°C can be provided with a reservoir depth of 4 km. However, in the case that an old existing DHS requires significantly higher supply temperatures, the required reservoir depth would increase significantly, which would come along with challenges for the drilling technology. However, considering the current trend to lower DHS supply temperatures suggests that this aspect would be only an obstacle for a low number of potential future projects. Furthermore, the practical implementation of advanced CHP configurations, such as Option II, increases the complexity of the plant construction and plant operation significantly compared with a sole-power generation system. These aspects should be considered within an improved thermo-economic evaluation and optimization considering improved and more accurate part-load models for the main components such as the turbine. Furthermore, the potential presence of a small amount of water in the CPG system (Fleming et al. [24]) might

[1] This price does not represent the retail price that is paid by the end-user within the district heating network but a business-to-business price between the operator of the CPG project and a DHS operator.

strongly affect the overall system's characteristic. On the one hand, the presence of water can significantly increase the achievable wellhead temperature, which is favourable with respect to the heat supply. On the other hand, the presence of water requires more complex plant layout and components. This applies to a potential separator and the design and manufacturing of CO_2 turbines. Thus, while the present work reveals that CPG systems can be favourable for CHP systems, further relevant aspects require more investigation with regard to a future commercial application.

Acknowledgements

Funding from the Bavarian State Ministry of Education, Science and the Arts in the framework of the Project Geothermal-Alliance Bavaria is gratefully acknowledged. In addition, the authors want to thank the editors and reviewers of the ECO2021 conference for suggesting this paper for the special issue. Parts of this work have been previously published as a conference paper within the ECOS2021 Proceedings [35].

Funding note

Open Access funding enabled and organized by Projekt DEAL.

References

[1] Lee I., Tester J.W., You F., Systems analysis, design, and optimization of geothermal energy systems for power production and polygeneration: State-of-the-art and future challenges. Renewable and Sustainable Energy Reviews, 2019, 109: 551–577.

[2] Aghahosseini A., Breyer C., From hot rock to useful energy: A global estimate of enhanced geothermal systems potential. Applied Energy, 2020, 279: 115769.

[3] Eyerer S., Schifflechner C., Hofbauer S., Bauer W., Wieland C., Spliethoff H., Combined heat and power from hydrothermal geothermal resources in Germany: An assessment of the potential. Renewable and Sustainable Energy Reviews, 2020, 120: 109661.

[4] Pan S.-Y., Gao M., Shah K.J., Zheng J., Pei S.-L., Chiang P.-C., Establishment of enhanced geothermal energy utilization plans: Barriers and strategies. Renewable Energy, 2019, 132: 19–32.

[5] Breede K., Dzebisashvili K., Liu X., Falcone G., A systematic review of enhanced (or engineered) geothermal systems: past, present and future. Geothermal Energy, 2013. DOI: 10.1186/2195-9706-1-4.

[6] Benim A.C., Cicek A., Eker A.M., A computational investigation of the thermohydraulics of an EGS Project. Journal of Thermal Science, 2018, 27(5): 405–412.

[7] Gao K., Liu W., Ma T., Hu Y., Fang T., Ye L., Numerical simulation study of a novel horizontally layered enhanced geothermal system: A case study of the Qiabuqia geothermal area, Qinghai Province, China. Journal of Thermal Science, 2021, 30(4): 1328–1340.

[8] Zhu J., Hu K., Zhang W., Lu X., A study on generating a map for selection of optimum power generation cycles used for Enhanced Geothermal Systems. Energy, 2017, 133: 502–512.

[9] Adams B., Fleming M.R., Bielicki J.M., Garapati N., Saar M.O., An analysis of the demonstration of a CO_2-based thermosiphon at the SECARB Cranfield Site. 46th Annual Stanford Geothermal Workshop (SGW 2021), Online, February 16–18, 2021. DOI: 10.3929/ethz-b-000467171.

[10] Brown D.W., A hot dry rock geothermal energy concept utilizing supercritical CO_2 instead of water. Proceedings of the Twenty-Fifth Workshop on Geothermal Reservoir Engineering, Stanford University, 2000, pp. 233–238.

[11] Randolph J.B., Saar M.O., Combining geothermal energy capture with geologic carbon dioxide sequestration. Geophysical Research Letters, 2011. DOI: 10.1029/2011GL047265.

[12] Adams B.M., Kuehn T.H., Bielicki J.M., Randolph J.B., Saar M.O., A comparison of electric power output of CO_2 Plume Geothermal (CPG) and brine geothermal systems for varying reservoir conditions. Applied Energy, 2015, 140: 365–377.

[13] Garapati N., Adams B.M., Fleming M.R., Kuehn T.H., Saar M.O., Combining brine or CO_2 geothermal preheating with low-temperature waste heat: A higher-efficiency hybrid geothermal power system. Journal of CO_2 Utilization, 2020, 42: 101323.

[14] Miranda-Barbosa E., Sigfússon B., Carlsson J., Tzimas E., Advantages from combining CCS with geothermal energy. Energy Procedia, 2017, 114: 6666–6676.

[15] Gupta N., Vashistha M., Carbon dioxide Plume Geothermal (CPG) System-A new approach for enhancing geothermal energy production and deployment of CCUS on large scale in India. Energy Procedia, 2016, 90: 492–502.

[16] Hansper J., Grotkamp S., Langer M., Wechsung M., Adams B.M., Saar M.O., Assessment of performance and costs of CO_2 Plume Geothermal (CPG) Systems. European Geothermal Congress, 2019.

[17] Goetzl G., Milenic D., Schifflechner C., Geothermal-DHC, European research network on geothermal energy in heating and cooling networks. Proceedings World Geothermal Congress 2020+1.

[18] Eyerer S., Dawo F., Schifflechner C., Niederdränk A., Spliethoff H., Wieland C., Experimental evaluation of an

ORC-CHP architecture based on regenerative preheating for geothermal applications. Applied Energy, 2022, 315: 119057.

[19] Chávez O., Godínez F., Polygeneration study of low-to-medium enthalpy geothermal reservoirs in Mexico. Journal of Thermal Science, 2021, 30: 1077–1087.

[20] Schifflechner C., Kaufmann F., Irrgang L., Kuhnert L., Dawo F., Wieland C., et al., Evaluation of plant configurations for geothermal trigeneration systems with organic Rankine Cycles. In: Technical University of Munich, editor. Proceedings of the 6th International Seminar on ORC Power Systems, 2021. DOI: 10.14459/2021mp1632994.

[21] Gladysz P., Pajak L., Sowizdzal A., Miecznik M., CO_2 enhanced geothermal system for heat and electricity production – process configuration analysis for central Poland. Proceedings of ECOS, 2019.

[22] Gladysz P., Sowiżdżał A., Miecznik M., Pająk L., Carbon dioxide-enhanced geothermal systems for heat and electricity production: Energy and economic analyses for central Poland. Energy Conversion and Management, 2020, 220: 113142.

[23] Schifflechner C., Dawo F., Eyerer S., Wieland C., Spliethoff H., Thermodynamic comparison of direct supercritical CO_2 and indirect brine-ORC concepts for geothermal combined heat and power generation. Renewable Energy, 2020, 161: 1292–1302.

[24] Fleming M.R., Adams B.M., Kuehn T.H., Bielicki J.M., Saar M.O., Increased power generation due to exothermic water exsolution in CO_2 Plume Geothermal (CPG) power plants. Geothermics, 2020, 88: 101865.

[25] Adams B.M., Kuehn T.H., Bielicki J.M., Randolph J.B., Saar M.O., On the importance of the thermosiphon effect in CPG (CO_2 plume geothermal) power systems. Energy, 2014, 69: 409–418.

[26] Sudhoff R., Glos S., Wechsung M., Adams B., Saar M.O., Next Level Geothermal Power Generation (NGP) – A new sCO_2-based geothermal concept. Proceedings of the German Geothermal Congress 2019. DOI: 10.3929/ethz-b-000449693.

[27] MATLAB. Version R2019b. Natick, Massachusetts: The MathWorks Inc., 2019.

[28] Lemmon E., Bell I., Huber M., McLinden M., NIST Standard Reference Database 23: Reference Fluid Thermodynamic and Transport Properties-REFPROP, Version 10.0, National Institute of Standards and Technology, 2018.

[29] Atrens A.D., Gurgenci H., Rudolph V., Electricity generation using a carbon-dioxide thermosiphon. Geothermics, 2010, 39(2): 161–169.

[30] Schifflechner C., Dawo F., Eyerer S., Wieland C., Spliethoff H., Combined heat and power generation by enhanced geothermal systems: Comparison of direct and indirect concepts for water and supercritical CO_2 as heat carriers. 5th International Seminar on ORC Power Systems, Athens, Greece, 2019.

[31] Gabbrielli R., A novel design approach for small scale low enthalpy binary geothermal power plants. Energy Conversion and Management, 2012, 64: 263–272.

[32] Dawo F., Wieland C., Spliethoff H., Kalina power plant part load modeling: Comparison of different approaches to model part load behavior and validation on real operating data. Energy, 2019, 174: 625–637.

[33] Lund H., Werner S., Wiltshire R., Svendsen S., Thorsen J.E., Hvelplund F., et al., 4th Generation District Heating (4GDH): Integrating smart thermal grids into future sustainable energy systems. Energy, 2014, 68: 1–11.

[34] Heberle F., Brüggemann D., Exergy based fluid selection for a geothermal Organic Rankine Cycle for combined heat and power generation. Applied Thermal Engineering, 2010, 30(11–12): 1326–1332.

[35] Schifflechner C., Wieland C., Spliethoff H., Thermodynamic and economic optimization of CO_2 Plume Geothermal Systems for combined heat and power production. The 34th International Conference On Efficiency, Cost, Optimization, Simulation and Environmental Impact of Energy Systems. Taormina, Italy, 2021. DOI: 10.52202/062738-0066.